Rohith Narra was a REU student at the University of Memphis, Department of Physics and Materials Science during Summer 2021. A junior from the University of Texas at Dallas, Rohith is pursing degrees in physics and chemistry. Upon finishing undergraduate studies, he seeks to pursue a Ph.D. in Applied Physics or Electrical Engineering specializing in Nanophotonics, and then become an industrial research associate.

Rohith Narra

Utilizing Silver Nanocubes to Promote Förster Resonance Energy Transfer (FRET) Between Cadmium Selenide and Perovskite Quantum Dots Embedded in a Polymer Layer Upon Optical Excitation

Faculty Sponsor

Dr. Thang B. Hoang

Abstract

In this work, we investigate the physical consequences of integrating a metal optical cavity into a mixed quantum dot donor-acceptor embedded in a polymer layer. The metal optical cavity is composed of silver nanocubes and the positively charged polymer PAH, and the quantum dots used are perovskite quantum dots emitting at 530 nm and CdSe/ZnS quantum dots emitting at 635 nm which are embedded in a PMMA layer. The system is optically excited with a 475 nm beam of varying power, and we seek to investigate whether the metal optical cavity is successful in promoting Forster Resonance Energy Transfer (FRET) between the quantum dots and if so with what efficiency. Based on the results, we will further improve the engineering of the system's electromagnetic environment. The implications of this research extend to nanophotonic devices and next generation opto-electronics through the conversion of incident infrared or UV photons into visible light.

Introduction

Quantum dots are semiconductor particles that are 1-10 nm in diameter, and they exhibit distinctive optical and electronic properties. Consequently, they hold applications in a variety of areas including in the context of quantum dot-based light-emitting diodes in photonics, replacing organic dyes for fluorescence-based sensing in biomedical science, and increasing the efficiency of photovoltaic cells when incorporated into their design. In order to understand how quantum dots are able to enjoy such unique characteristics, their electronic structure and the effect of quantum confinement must be examined.

The highest energy electrons within the quantum dot exist in the outermost electronic orbital which is known as the valence band. These electrons become conductive once supplied with enough energy to exit the valence band and enter the conduction band, and this energy difference is known as the "bandgap". When an electron in the valence band is promoted into the conduction band, it leaves behind a mobile positively charged vacancy in the valence band known as a "hole" and forms an electron-hole pair. The electron and its hole are bound by coulombic interactions to form a quasiparticle known as an "exciton" and will thus recombine once the electron drops back down into the valence band which results in photon emission [5]. This entire process is known as photoluminescence (PL).

The wavelength of the light emitted upon exciton recombination is dependent upon the bandgap which is related to the size of the quantum dot due to quantum confinement. Specifically, as the size of the quantum dot decreases, the distance between the electron-hole pair decreases which results in more energy being required to separate the exciton pair for photoluminescence and results in a "blue shift" (lower wavelength) in emission [5]. To accurately measure the wavelength of peak emission of a particular type of quantum dot, one would perform PL spectroscopy on a sample that generates a PL spectrum – a plot of intensity (counts) as a function of wavelength (nm). When two different types of quantum dots are in close proximity together, the type which emits at a lower wavelength and the type which emits at a higher wavelength may serve as an energy donor and energy acceptor respectively upon optical excitation of the donor in certain energy transfer processes such as FÖrster Resonance Energy Transfer (FRET).

FRET is a non-radiative energy transfer from an excited fluorescent donor to a lower energy acceptor, and the driving force for this energy transfer is long range dipole-dipole interactions [1]. The chief requirement for FRET to occur between a donor-acceptor pair is spectral overlap between the emission spectrum of the donor with the absorbance spectrum of the

acceptor, and it must be noted that FRET is a highly distance-dependent phenomenon as the efficiency of the FRET process is directly proportional to $1/r^6$ where r is the distance between the acceptor and donor. The first step of FRET is excitation of the donor which forms a dipole that oscillates and dissipates energy during "vibrational relaxation" which occurs in the course of picoseconds [4]. The donor is then oscillating at an energy equivalent to the electronic energy gap of its excited state. In order for the resonance energy transfer to occur, the excited donor must be oscillating at a frequency resonant with the ground state electronic energy gap of the acceptor [4]. Once the energy transfers to the acceptor, vibrational relaxation followed by emission from the acceptor take place [4]. This can be observed from the PL spectrum following FRET where a spectral shift occurs – The height of the donor's peak decreases and the height of the acceptor's peak increases [4]. Another expected observation is from Time-Correlated Single Photon Counting (TCSPC) measurements where the decay times of the emitted photons are measured – the lifetimes of the photons emitted by the donor should decrease due to the nonradiative energy transfer process.

Suppose there is insufficient overlap between donor's emission and acceptor's absorbance spectrum for FRET to take place, the FRET effect will be negligible. To enhance the FRET effect, one would need to improve the spectral overlap between the appropriate spectra for the donor and acceptor. Furthermore, the donor's spontaneous emission can also be enhanced with an additional component in the system by the Purcell effect – the rate at which a quantum system spontaneously emits increases following modifications to its photonic environment as it increases the photonic density of states [2]. For example, researchers from Henan University demonstrated that metal-optical nanocavities (composed of silver nanocubes and PVP layer) when coupled to perovskite quantum dots (PQD) were able to enhance the spontaneous emission of the PQDs by nearly 3.5-fold [3]. Thus, incorporating metal-optical cavities into a donor-acceptor system with little spectral overlap should, in principle, increase the likelihood of FRET taking place between the two by bridging the gap.

Experimental Methods

In our setup, we incorporated silver nanocubes that act as plasmonic nanoparticles. They are meant to bridge the gap between donor and acceptor. All four of our samples consist of the donor-acceptor system consisting of PQDs (donor) and CdSe QDs (acceptor) embedded in a poly (methyl methacrylate) (PMMA) monolayer bound to a glass substrate. Of those four, two included, the silver nanocubes as well, and one of those two include

a poly (allylamine hydrochloride) (PAH) monolayer bound to the silver nanocubes forming a complete metal-optical cavity. We then checked for the presence of the FRET effect along with its strength in each sample upon optical excitation with a 475 nm beam with varying power.

The quantum dots used were supplied by Sigma Aldrich with the CdSe/ZnS quantum dots emitting at 635 nm (731870) and the Perovskite quantum dots emitting at 530 nm (905062). Additionally, the 100 nm Ag nanocubes were supplied by Nanocomposix (NCXSCPH100) and the PMMA solution was supplied by Kayaku Advanced Materials. The PAH solution was prepared by dissolving 132 mg of PAH powder and 29 g of NaCl in 500 mL of DI H2O. Other materials involved in sample assembly included glass slides, plastic strips, microcentrifuge conical tubes, and 20-200 uL pipette with the corresponding tips. The instruments and apparatuses used in sample assembly were a glass cutter, forceps, double-sided tape, sample containers, spin coater, sonicator, and vortex machine. After assembly, the samples were put in "dark" storage until we optically excited them with a Ti: Sapphire laser. The PL spectra were collected by our Horiba spectrometer. The TCSPC data was collected with our Pico quant Time-Correlated Single Photon Counting apparatus, and the data is then analyzed with the Easy Tau software.

With regards to sample assembly, first four sample containers were gathered, labeled by sample number, and a strip of double-sided tape was placed inside each container. Then, four square-shaped glass slides were cut, and three different quantum dot-polymer mixtures were prepared via quantitative transfers and stored in separate microcentrifuge conical tubes. Solution 1 was used in preparing sample 1, and it consists of 200 μL of colloidal perovskite quantum dots (PQD) solution diluted with the 200 μL of PMMA solution. Solution 2 was used in preparing sample 2, and it consists of 200 μL of colloidal CdSe quantum dots (CdSe QD) solution diluted with 200 μL of the PMMA solution. Solution 3 was used in preparing samples #3 and #4, and it consists of 150 μL of solution 1 mixed with 150 μL of solution 2. All three solutions were blended via vortexing and sonication.

To prepare sample 1, 100 μL of solution 1 was pipetted unto one of the glass pieces. Then, the glass piece with the solution was placed on the spin-coater's rotating drum and then spun at 1,000 rpm for one minute to create the monolayer. Finally, the glass slide was placed on the tape in the sample container with forceps. The same process was repeated for samples 2, 3, and 4 except with solutions 2 and 3 respectively. Prior to taking optical measurements, 75 μL of Ag nanocubes are pipetted unto a plastic piece and touched against the sample 4 slide for fifteen minutes to allow the nanocubes to bind. Then, the slide was submerged in the PAH solution for five minutes

to form another monolayer above the nanocubes, sandwiching them with the PMMA monolayer.

Sample #	Constituents
1	Perovskite Quantum Dots (PQD), and PMMA
2	Cadmium Selenide Quantum Dots (CdSe), and PMMA
3	PQD, CdSe, PMMA, and PAH
4	PQD, CdSe, PMMA, PAH, and Ag Cubes

Table 1. Sample Components

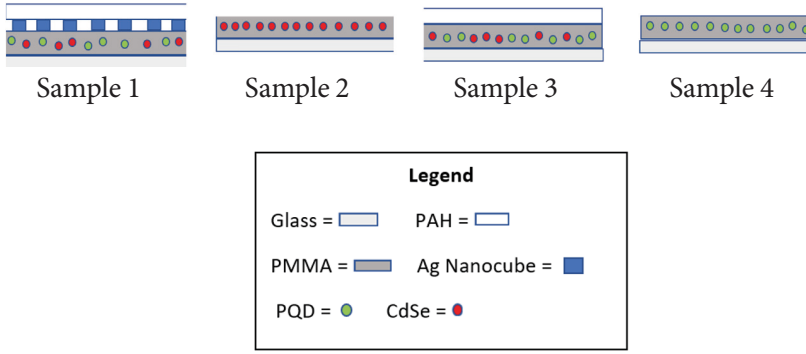

With regards to optical measurements, the sample was first placed on the sample holder which was set up on top of the light microscope's stage. Then, the sample was viewed under the microscope to ensure that the correct side will interact with the beam. The Ti: Sapphire laser was tuned to emit a light beam with a wavelength of 970 nm that passes through a second harmonic generation apparatus to reduce the beam's wavelength to 485 nm. An optical path (system of mirrors and lenses was set up) on the optics table such that the incoming beam hit the sample at the desired position with reasonable intensity. Next, a PL spectrum was recorded to verify that each emitter is active in the sample and then upon verification, TCPSC measurements were taken scanning between 502 nm and 690 nm with a scan taken every five nanometers. The collection time for PL spectroscopy was ninety seconds and fifteen seconds per scan for TCSPC. This procedure was repeated for each laser power tested per sample. In addition to taking TCSPC measurements for all four samples, a scan of the laser hitting a gold piece on the sample stage was taken to obtain the instrument response function (IRF) which was used later when performing curve fitting of the decay curves.

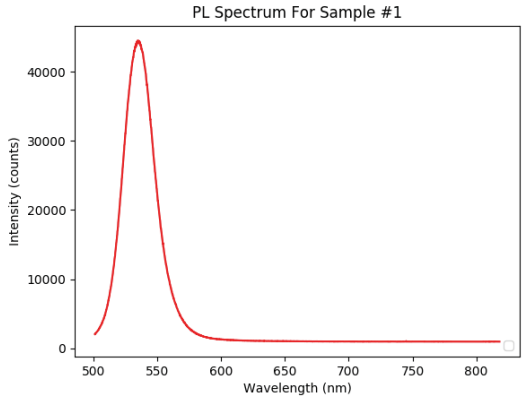

Figure 1. Sample 1's PL spectrum (537 nm max)

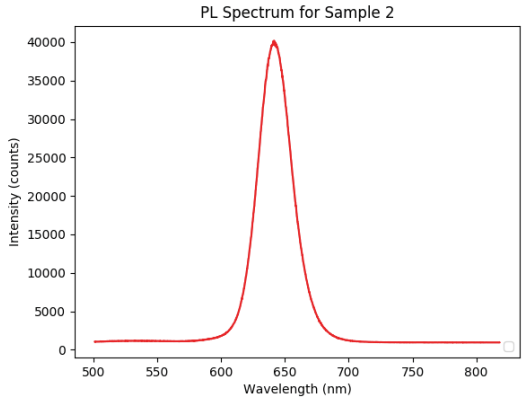

Figure 2. Sample 2's PL spectrum (632 nm max)

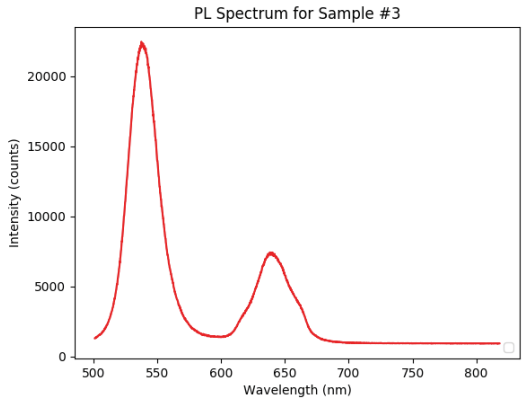

Figure 3. Sample 3's PL spectrum

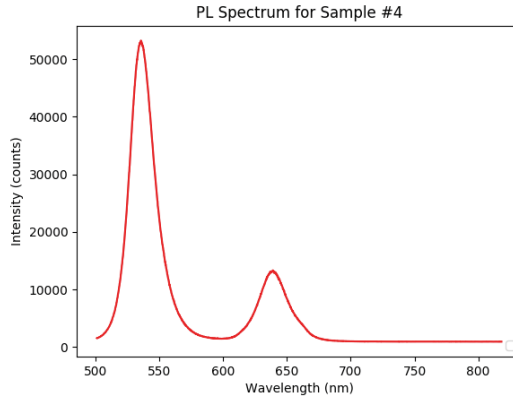

Figure 4. Sample 4's PL spectrum

Results

Even though decay spectra were collected between wavelengths containing each peak, the decay times were measured for the photons of wavelengths in a 20 nm range where the middle of that range is the peak wavelength. For samples 1, 3, and 4, we measured the decay times for the PQD emission photons in the range between 527 nm and 547 nm. For samples 2, 3, and 4, we measured the decay times for the CdSe QD emission photons in the range between 622 nm and 642 nm. To obtain the decay times for the relevant wavelengths, we performed nonlinear curve fitting of the respective decay spectra using the Easy Tau software. The fit we performed was an "exponential reconvolution" fit where the IRF is deconvoluted from the decay curve and fitted to one term which is $I_1 e^{-t}/T$ where I_1 is the peak intensity, *t* is time, and T is the decay time. Upon obtaining the desired decay times, we then calculated the mean decay times in each range with standard error of the mean per sample.

Sample #	PQD Wavelengths Mean Decay Time (ns)	Standard Error of Mean (ns)
1	95.06	11.68
3	69.77	3.29
4	108.64	10.86

Table 2. Mean decay times for PQD emission photons for samples containing PQDs at lower powers (2 uW or 10 uW)

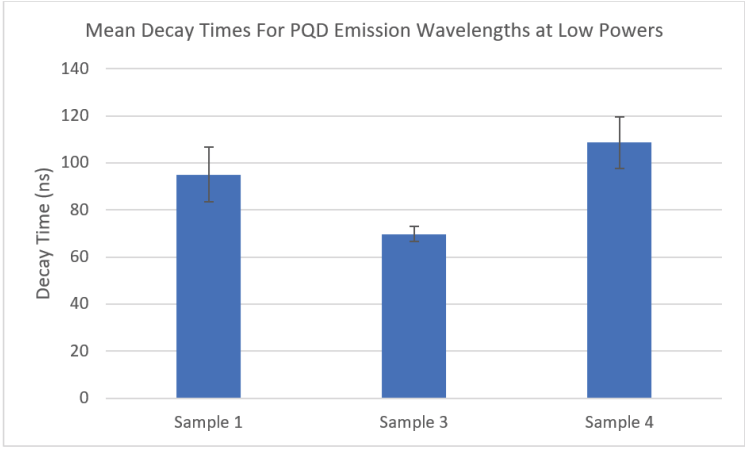

Figure 5. Mean decay times for PQD at lower powers (2 uW or 10 uW)

Sample #	PQD Wavelengths Mean Decay Time (ns)	Standard Error of Mean (ns)
1	47.72	5.33
3	55.68	2.78
4	73.95	1.50

Table 3. Mean decay times for PQD emission photons for samples containing PQDs at higher powers (5 uW or 20 uW)

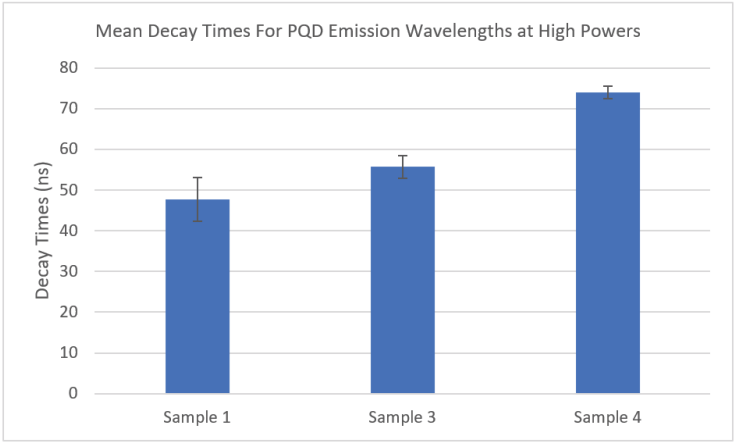

Figure 6. Mean decay times for PQD at higher powers (5 uW or 20 uW)

Sample #	CdSe Wavelengths Mean Decay Time (ns)	Standard Error of Mean (ns)
2	23.43	0.79
3	29.17	0.80
4	27.10	0.41

Table 4. Mean decay times for CdSe emission photons for samples containing CdSe QDs at 10 uW power

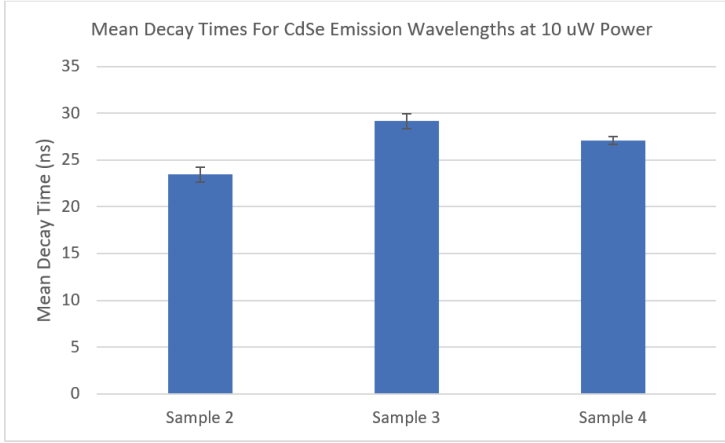

Figure 7. Mean decay times for CdSe QDs at 10 uW power

Sample #	CdSe Wavelengths Mean Decay Time (ns)	Standard Error of Mean (ns)
2	23.10	1.10
3	21.09	0.86
4	24.44	0.61

Table 5. Mean decay times for CdSe emission photons for samples containing CdSe QDs at 20 uW power

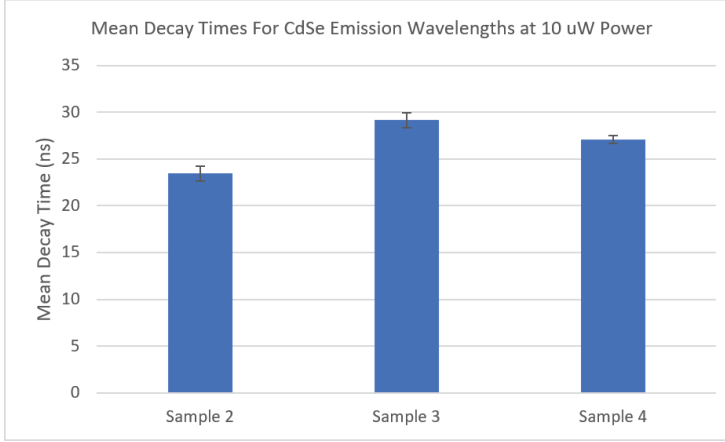

Figure 8. Mean decay times for CdSe QDs at 20 uW

One sample was prepared for each sample number, but multiple data points were acquired for statistical analysis by testing each sample at different laser powers. The PL spectra were taken once for each sample, and the data points were the mean decay time for the relevant photons at each power. The degrees of freedom per test varied between four to six degrees depending on the quality of the TCSPC data acquired for a sample at a given power. As the silver nanocubes were meant to enhance the emission of the perovskite quantum dots and promote FRET between the donor-acceptor pair, two sample t-tests assuming unequal variances were performed using Microsoft Excel's Data Analysis package on the decay time data comparing:

Sample 1 vs Sample 4 for PQD emission for both lower and higher powers

Sample 3 vs Sample 4 for PQD emission for both lower and higher powers

Below are the results of the t-tests including the statistical conclusions to be drawn:

Null Hypothesis (H_0)	$T_{sample\ 1} = T_{sample\ 4}$
Alternative Hypothesis (H_A)	$T_{sample\ 1} < T_{sample\ 4}$
Test Statistic	-0.851936
P-Value	0.2095103
Statistical Conclusion	Accept H_0 at significance of 0.05

Table 6. Two sample one-sided t-test results for comparison of Samples 1 and 4's PQD decay times at lower powers

Null Hypothesis (H_0)	$T_{sample\ 1} = T_{sample\ 4}$
Alternative Hypothesis (H_A)	$T_{sample\ 1} < T_{sample\ 4}$
Test Statistic	-4.735716
P-Value	0.0025849
Statistical Conclusion	Reject H_0 and accept H_A at significance of 0.05

Table 7. Two sample one-sided t-test results for comparison of Samples 1's and 4's PQD decay times at higher powers

Null Hypothesis (H_0)	$T_{sample\ 3} = T_{sample\ 4}$
Alternative Hypothesis (H_A)	$T_{sample\ 3} < T_{sample\ 4}$
Test Statistic	-3.426882
P-Value	0.0093492
Statistical Conclusion	Reject H_0 and accept H_A at significance of 0.05

Table 8. Two sample one-sided t-test results for comparison of Samples 3's and 4's PQD decay times at 10 uW power

Null Hypothesis (H_0)	$T_{sample\ 3} = T_{sample\ 4}$
Alternative Hypothesis (H_A)	$T_{sample\ 3} < T_{sample\ 4}$
Test Statistic	-5.7879297
P-Value	0.000582
Statistical Conclusion	Reject H_0 and accept H_A at significance of 0.05

Table 9. Two sample one-sided t-test results for comparison of Samples 3's and 4's PQD decay times at 20 uW power

Two sample t tests assuming unequal variances were also performed on the decay time data comparing:

Sample 2 vs Sample 4 for CdSe QD emission for 10 uW and 20 uW

Sample 3 vs Sample 4 for CdSe QD emission for 10 uW and 20 uW

Null Hypothesis (H_0)	$T_{sample\ 2} = T_{sample\ 4}$
Alternative Hypothesis (H_A)	$T_{sample\ 2} < T_{sample\ 4}$
Test Statistic	-4.10654
P-Value	0.003155
Statistical Conclusion	Reject H_0 and accept H_A at significance of 0.05

Table 10. Two sample one-sided t-test results for comparison of Samples 2's and 4's CdSe QD decay times at 10 uW power

Null Hypothesis (H_0)	$T_{sample\ 2} = T_{sample\ 4}$
Alternative Hypothesis (H_A)	$T_{sample\ 2} < T_{sample\ 4}$
Test Statistic	-1.06847
P-Value	0.163201
Statistical Conclusion	Accept H_0 at significance of 0.05

Table 11. Two sample one-sided t-test results for comparison of Samples 2's and 4's CdSe QD decay times at 20 uW power

Null Hypothesis (H_0)	$T_{sample\ 3} = T_{sample\ 4}$
Alternative Hypothesis (H_A)	$T_{sample\ 3} > T_{sample\ 4}$
Test Statistic	2.300064
P-Value	0.030548
Statistical Conclusion	Reject H_0 and accept H_A at significance of 0.05

Table 12. Two sample one-sided t-test results for comparison of Samples 3's and 4's CdSe QD decay times at 10 uW power

Null Hypothesis (H_0)	$T_{sample\ 3} = T_{sample\ 4}$
Alternative Hypothesis (H_A)	$T_{sample\ 3} < T_{sample\ 4}$
Test Statistic	-3.19702
P-Value	0.007564
Statistical Conclusion	Reject H_0 and accept H_A at significance of 0.05

Table 13. Two sample one-sided t-test results for comparison of Samples 3's and 4's CdSe QD decay times at 20 uW power

Discussion and Conclusion

Based on the observations stated above, we can conclude that the silver nanocubes did not succeed in promoting FRET between the donor-acceptor system as the Purcell effect dominated the FRET effect in our setups. If FRET had occurred, an acceptor peak taller than the donor peak on the PL spectrum for sample #4 would have been observed. Also, the mean decay times of both PQD and CdSe QD emissions should have decreased. Regardless of these results, future experiments could be performed in which one alters the amount of each constituent and assess how successful they would be at promoting FRET.

Specifically, we could perhaps observe what occurs when we reduce the spatial density of the silver nanocubes on the QD-PMMA monolayer in order to obtain the desired Purcell enhancement without it dominating the overall FRET effect or we could prepare different samples where we vary the donor to acceptor ratios. Another avenue which could be explored is integrating another plasmonic structure into our sample designs such as a gold or silver sheet to increase the likelihood of the dipole-dipole coupling needed for FRET due to enhanced dielectric effects upon optical excitation

From the PL spectrum for sample #4, there was no decreasing of the donor peak and increasing of the acceptor peak which is the first indication that FRET may not have occurred between the PQDs and CdSe QDs. Still, the decay data must be examined to draw any definite conclusions. At higher powers, there was statistically significant Purcell enhancement of the PQD's for sample #4 when compared to sample #1 but not at lower powers. At both lower and higher powers, there was statistically significant Purcell enhancement of the PQD's for sample #4 when compared to sample #3. From this, we can state that the silver nanocubes did indeed succeed in promoting increased spontaneous emission from the donor. With regards to CdSe emission, no consistent trends could be observed because all outcomes were represented roughly equal in the data.

Acknowledgements

I would like to first thank the National Science Foundation for funding me, and I would like to extend my gratitude to Dr. Hoang, Bryson Krause, and Jolaikha Sultana for impeccable mentorships. Finally, thanks also go to Dr. Firouzeh Sabri for making the arrangements for us students to get the most out of the University of Memphis Physics REU program.

References

[1] Chou, K., & Dennis, A. (2015). Förster resonance energy transfer between quantum DOT donors and quantum DOT ACCEPTORS. Sensors, 15(6), 13288–13325. https://doi.org/10.3390/s150613288

[2] Hoang, T. B., Akselrod, G. M., Argyropoulos, C., Huang, J., Smith, D. R., & Mikkelsen, M. H. (2015). Ultrafast spontaneous emission source using plasmonic nanoantennas. Nature Communications, 6(1). https://doi.org/10.1038/ncomms8788

[3] Li, H., He, F., Ji, C., Zhu, W., Xu, Y., Zhang, W., Meng, X., Fang, X., & Ding, T. (2019). Purcell-Enhanced spontaneous emission From PEROVSKITE quantum Dots coupled to Plasmonic Crystal. The Journal of Physical Chemistry C, 123(41), 25359–25365. https://doi.org/10.1021/acs.jpcc.9b06919

[4] Libretexts. (2020, August 15). Fluorescence. Chemistry LibreTexts. https://chem.libretexts.org/Bookshelves/Physical_and_Theoretical_Chemistry_Textbook_Maps/Supplemental_Modules_(Physical_and_Theoretical_Chemistry)/Spectroscopy/Electronic_Spectroscopy/Radiative_Decay/Fluorescence.

[5] Parak, W. J., Manna, L., & Nann, T. (2010). Fundamental principles of quantum dots. Nanotechnology. https://doi.org/10.1002/9783527628155.nanotech004